Journal of Photochemistry and Photobiology A: Chemistry 204 (2009) 90–96

Contents lists available at ScienceDirect

Journal of Photochemistry and Photobiology A: Chemistry

journal homepage: www.elsevier.com/locate/jphotochem

Spectroscopic and quantum chemical study of the Brønsted acid sites in zeolite L channels with acidochromic cyanine dyes

Beate Bussemer*, Ines Dreiling, Ulrich-Walter Grummt, Gerhard. J. Mohr

Institute of Physical Chemistry, Friedrich-Schiller University Jena, Lessing Street 10, D-07743 Jena, Germany

ARTICLE INFO

Article history:
Received 20 November 2008
Received in revised form 12 January 2009
Accepted 23 February 2009
Available online 9 March 2009

Keywords:
Acidochromic phenolbetaine
Solvatochromism
Fluorescent dyes
Amine probe

ABSTRACT

Four pH sensitive cyanine dyes with pK_a values (in aqueous solution) of 3.4, 5.0, 6.8, and 8.6 were inserted into the pores of zeolite L to estimate the acidity of the zeolite channels. The photophysical properties of the dyes were investigated first in solution via UV–vis and fluorescence spectroscopy. The absorption and the emission maxima of the protonated and deprotonated forms vary significantly for all dyes, with the protonated forms absorbing at around 350 nm, and the deprotonated forms at around 450 nm. In the channels of zeolite L the two dyes with the higher pK_a values were completely protonated, while the two dyes with lower pK_a values were partially deprotonated. We found a pH value between 3.0 and 3.5 inside the pores of a fully hydrated potassium exchanged zeolite L. Preliminary results show that the zeolite particles can also be used to probe gaseous amines from aqueous solutions.

DFT cluster optimizations were carried out to study the Brønsted acidity of the zeolite pore. Acidity was related to the hydrogen bond strength of the zeolite, which was characterized by geometric parameters, and by adsorption energy. The optimizations showed an interaction between the dye and the acid site of the zeolite. This interaction caused a change in the dye structure and the position of the proton.

1. Introduction

The concentration estimation of ions or small biomolecules plays an important role in medical and biological experiments. Fluorescent indicator dyes in particular are valuable tools for measuring changes in intracellular ion concentration by providing the necessary sensitivity required for optical measurements inside living cells [1,2]. The investigation of living cells or tissues makes high demands on the sensors with regards to their biocompatibility and mechanical stability. To avoid direct contact with the cytosol, and to decrease the risk of destroying the cells, embedding of the sensor dye into an inert matrix is a widely used method. Another advantage of the embedding technique is the undisturbed reaction between the fluorescent dye and the analyte that is free of any non-specific binding with biomolecules. Modern nanosensors contain a sensor unit embedded into a biologically inert polymer matrix [3,4]. In relation to these materials, host–guest systems based on zeolites are particularly attractive [5]. They offer a well-defined microenvironment to the dyes, and the particle size can easily be adjusted to the particular need. The large variety of molecular sieves featuring different pore structures and morphologies offers multiple possibilities for the design of host–guest systems with specific properties. Due to their particular structure and chemical properties (i.e. their well-defined pore structure and amphoteric interface), zeolite–dye systems have been used to develop advanced materials with unique optical properties. The possibility to organize dye molecules within the zeolite matrix at a supramolecular level has been used to develop artificial optical antenna [6], solid tunable lasers [7], and new materials for non-linear optics applications.

While embedding dyes in zeolite structures offers shielding from the local environment, the photophysical behavior of dyes is often changed after insertion into zeolite pores [8]. The interaction between the guest molecules and the zeolite Brønsted sites is one contribution to this change. Furthermore, interactions between the dyes and co-cations play a role. These interactions are strong in absence of a solvent inside the channels. In the presence of a solvent, the counterions are solvated and their interactions with the encapsulated molecules are weakened. With fully hydrated zeolite samples the interaction between the Brønsted sites and dyes becomes predominant [9]. At high dye loading, the spectra can also be influenced by J-aggregation of the molecules or by self-absorption [10].

A detailed knowledge of the pore properties and their impact on the dye's absorption and emission behavior is a prerequisite to the development of new combined dye–zeolite materials. A characteristic pore property is the acidity of the channels. It depends on the zeolite type, on the Si:Al ratio, and on the kind of the

* Corresponding author. Tel.: +49 3641 948323; fax: +49 3641 948302.
E-mail address: beate.bussemer@uni-jena.de (B. Bussemer).

1010-6030/$ – see front matter © 2009 Elsevier B.V. All rights reserved.
doi:10.1016/j.jphotochem.2009.02.017

counter cations. The influence of the counterions can be explained by acid–base reactions with water. Metal cations give acidic solutions when dissolved in water. The pH changes dependent on the nature of the counterion were recently reported in [9]. The acidic proton is usually located at one of the four oxygen atoms in the vicinity of the negatively charged aluminum. It can move from one oxygen atom to another, and its mobility is greatly increased in the presence of H_2O, or by heating [11].

A variety of different analytical and spectroscopic techniques have been made available for acidity characterization of solid acids. One approach to investigating the proton activity, or acidity, has been to consider protonated sites within the bare unloaded zeolite. This has led to a number of experimental and theoretical studies of proton mobility, and of deprotonation energies, as methods of quantifying acidity [12,13]. Here, increased acidity can be related to greater proton mobility and/or lower proton affinity. An alternative approach involves the interaction of inserted molecules with the Brønsted sites to investigate the actual acidity experienced by a given molecule. Quantum mechanical calculations [14,15] and experimental studies, such as microcalorimetry [16,17], solid-state NMR spectroscopy [18,19], temperature-programmed desorption [20,21], and vibrational and electronic spectroscopy [22–26] have concentrated on these interactions. Among those, obtaining the proton activity inside the zeolite channels by measuring the ratio of protonated and unprotonated dye by means of spectroscopic methods is particularly attractive [9].

We present in this work a dye–zeolite material composed from acidochromic phenolbetaine dyes (Fig. 1a–c) incorporated into the pores of zeolite L. Their absorbance and dissociation behavior is strongly influenced by the electron donor and acceptor substituents on the chromophore [27–29]. Furthermore, for comparison, we also used a stilbazolium salt (Fig. 1d) whose incorporation into the pores of zeolite X, Y, and L has been described elsewhere [6,9,30]. Deprotonation of these dyes results in an enlarged π electron system compared to the protonated dyes. For this reason the absorption maximum of the deprotonated forms is shifted to longer wavelengths. First we investigated the spectral and dissociation behavior of the dyes in aqueous solution and estimated their pK_a values. After insertion of the dyes in the zeolite the magnitude of protonation was investigated via remission and fluorescence spectroscopy. Due to the strong interaction of the encapsulated dyes with the zeolite channels, dye exchange can almost be excluded and the zeolite material is only able to exchange small molecules, small cations or solvents.

The possible use of the fluorescent zeolite as a sensor material was tested through reaction with amines.

The electronic spectra of phenolbetaine dyes strongly depend on the polarity of their microenvironment and exhibit negative solvatochromism [31]. This behavior indicates that the ground state of the dyes is much more polar than its excited state, and acquires extra stabilization with increased polarity of the solvent. Measuring the solvatochromism of the dyes in several solvents gives an insight to the polarity of the zeolite L pores by comparing the spectra of the dyes in solution and in the zeolite.

Quantum chemical calculations were carried out on clusters representing the individual Brønsted sites in the chosen structures interacting with the dye molecules. The cluster models were carefully selected to model the Brønsted site, as well as significant portions of the neighboring zeolite pore system. A range of geometries and energies are presented and discussed. Acidity in the sorption complexes is characterized from the hydrogen bond strength, as measured by the O–H, or N–H, distances, respectively. Here, we use the hydrogen-bond strength as a descriptor of acidity, with greater hydrogen bond strength being related to stronger acidity.

2. Experimental

2.1. Chemicals and reagents

4-[2-(4-Hydroxyphenyl)-vinyl]-1-methylpyridinium bromide and *4-[2-(4-Dimethyl-aminophenyl)-vinyl]-1-methylpyridinium iodide* (**ST1** and **ST4**, Fig. 1a and d) were purchased from Aldrich.

4-[2-(3-Bromo-4-hydroxy-5-methoxyphenyl)-vinyl]-1-methylpyridinium bromide (**ST2**, Fig. 1b):

The dye was obtained by dissolving 1.70 g of 5-bromovanillin and 1.55 g of 1,4-dimethylpyridinium bromide in 20 ml of warm methanol and then adding 1.0 ml of piperidine. The mixture was refluxed for 6 h, cooled to room temperature and the resulting precipitate washed with 100 ml of cold methanol. The product was re-crystallized from a mixture of methanol/water (9:1) to give the deprotonated chinoid derivative. This derivative (0.5 g) was dispersed in 10 ml methanol, and 1.0 ml of 48% hydrobromic acid was added to protonate the dye. The yellow dispersion was filtered and washed with 5 ml of cold methanol to give 4-[2-(3-bromo-4-hydroxy-5-methoxyphenyl)-vinyl]-1-methylpyridinium bromide.

1H NMR: d (ppm): 8.83 (d, 2H), 8.13 (d, 2H), 7.90 (d, 1H), 7.38-7.52 (m, 3H), 4.27 (s, 3H), 3.92 (s, 3H).

MS: m/z = 305 (M—CH3—HBr).

4-[2-(3,5-Dibromo-4-hydroxyphenyl)-vinyl]-1-methylpyridinium bromide (**ST3** Fig. 1c):

Similar to the above procedure, the dye was obtained by reacting 2.00 g of 3,5-dibromo-4-hydroxybenzaldehyde with 1.55 g of 1,4-dimethylpyridinium bromide to give 4-[2-(3,5-dibromo-4-hydroxyphenyl)-vinyl]-1-methylpyridinium bromide.

1H NMR: d (ppm): 10.57 (s, 1H), 8.87 (d, 2H), 8.14 (d, 2H), 7.85-7.98 (m, 3H), 7.48 (d, 1H), 4.27 (s, 3H).

MS: m/z = 355 (M—CH3—HBr).

Zeolite L: The synthesis of the fully hydrated pure potassium form of zeolite L crystals ($K_9(AlO_2)_9(SiO_2)_{27}{\cdot}21H_2O$) was carried out according to the standard procedure under static conditions [6].

The dye–zeolite materials were prepared by cation exchange in an aqueous solution. For this, 500 mg of zeolite L was dispersed into 25 ml of an aqueous solution of 2.5 mg dye, and the mixture was heated to boiling point. To remove the dye molecules on the outer surface of the zeolite, 0.1 ml of acidic hypochloride solution was added to the dye–zeolite samples [24].

Thin layers containing the dye loaded zeolite probes were obtained by adding the respective zeolite probe to a solution of EVA33 (ethylene–vinylacetate copolymer with 33% vinylacetate) in 0.4 ml of THF. This suspension was spin-coated on a quartz plate that served as a mechanical support for the hybrid zeolite/polymer layer. The resulting layers were used to record the fluorescence spectra of the dye loaded zeolite.

2.2. Spectroscopic measurements

The absorption spectra of the dissolved acidochromic dyes, as well as the remission spectra of the zeolite powder, were recorded on the UV–vis–NIR Spectrometer CARY 5000 (Varian) $20 \pm 2\,^{\circ}C$. For the latter an external diffuse reflectance attachment (praying mantis) by Harrick was used [32].

All fluorescence spectra were recorded on a Luminescence Spectrometer LS50 (PerkinElmer).

The pK_a values of all dyes in aqueous solution were calculated from pH-dependent absorption data (cf. Fig. 3). The pH values were adjusted via a Sörensen phosphate buffer or a universal buffer.

To estimate the response of the inserted dye **ST3** to 1-propylamine, the dye–zeolite probe in powder form was placed on a quartz plate and mechanically fixed with a teflon layer. The microporous teflon is not permeable for ions and allows only unpro-

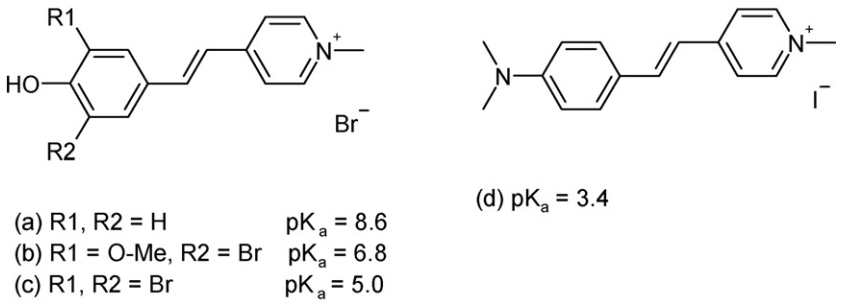

Fig. 1. Hydroxystilbazolium and aminostilbazolium dyes with different functional groups to influence their pK_a value. (a) **ST1**, (b) **ST2**, (c) **ST3**, (d) **ST4**.

tonated gaseous molecules to pass through. The quartz plate with the sensor layer was fixed in a custom-made flow-through cell. The fluorescence spectra were obtained by placing the flow-cell in the spectrometer (LS50) and pumping amine solutions through the cell at a flow rate of 2.3 ml min^{-1} using a peristaltic pump. We used various amine concentrations (8.5 mM, 17 mM, 85 mM, 170 mM, 850 mM) in a 0.1 M NaOH solution (pH 13). At this pH value the amine is deprotonated. Since 1-propylamine is highly volatile, gaseous neutral amine molecules can pass through the teflon layer and deprotonate **ST3** inside the zeolite pores. A quarternary ammonium salt, which is not volatile is formed through this reaction. The reaction was detected by the increase of the fluorescence intensity of the deprotonated form of the dye at an excitation wavelength of 450 nm. For each amine concentration, a time drive spectrum was first recorded at a constant emission wavelength of 610 nm until equilibrium in response to the gaseous amine was reached. Then the fluorescence spectrum was recorded. Furthermore, spectra with the pure NaOH solution, before and after the exposure to the amine, were recorded to test the reversibility of the reaction.

2.3. Quantum chemical calculations

Classical zeolites are built up by corner-sharing TO_4 tetrahedra (T:Si, Al). The substitution of a tetravalent silicon atom by a trivalent aluminum atom in a TO_4 unit creates a negative charge, which is then balanced by a cation. Exchange of a cation with a proton leads then to the formation of a Brønsted site with the proton located at a bridging oxygen atom between a silicon atom and an aluminum atom.

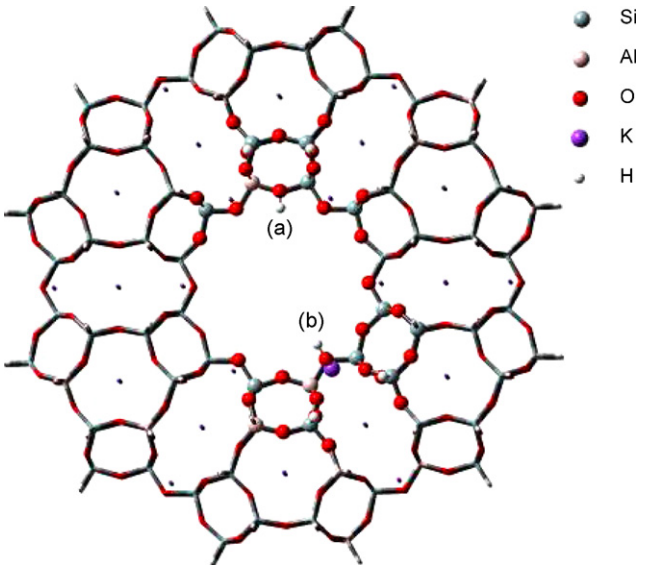

Fig. 2. View inside the channel of zeolite L, and the clusters chosen for quantum chemical calculations. (a) **Z1**, (b) **Z2**.

In the channels of zeolite L one can distinguish two different places where an acidic site can be formed. Fig. 2 shows a channel and the places of these sites. Two types of clusters were generated, with each of the clusters containing one acidic site, two coordination spheres of T sites around the proton carrying oxygen atom, and the cyanine dye under consideration. The number of T sites in the first cluster (Fig. 2a, **Z1**) is eight (7 Si, 1 Al). The second cluster (Fig. 2b, **Z2**) includes 12 T sites (10 Si, 2 Al) due to closing rings in the zeolite structure. Dangling bonds were saturated with hydroxy groups to keep the zeolite cluster neutral. To obtain a neutral zeolite cluster, a K^+ ion was exchanged by the proton. The proton was placed on an oxygen atom in an Al–O–Si unit that is directed into the zeolite pore. The initial OH radius chosen was 0.95 Å. The initial distance between the zeolite proton and the dye oxygen chosen was 2.0 Å. During the optimization all atoms were allowed to relax except the saturating H-atoms. For that reason it is not possible to calculate vibrational spectra without full optimization. The corresponding clusters without adsorbed dye were also optimized. All calculations were performed using GAUSSIAN 03 [33]. The B3LYP functional together with a 6-31g(d) basis set was used in all cases for optimization.

3. Results and discussion

3.1. pK_a value of the cyanine dyes

The dyes **ST1**—**ST4** show absorbance maxima between 330 and 375 nm for the acid forms and between 435 and 460 nm for the base forms (see Table 1). The absorbance spectra are well separated. Accordingly, the color changes of phenolbetaine dyes in going from acid to base form (i.e. protonated to deprotonated form) are from yellow to orange or red (Fig. 3).

The fluorescence maxima are between 408 and 609 nm for the acid forms and between 580 and 611 nm or the base forms (Table 1). In accordance with Lehmann et al. [28], the absorbance and fluorescence maxima of the protonated forms are shifted to shorter wavelengths in all cases. The corresponding spectra are given in Fig. 4.

The pK_a values are calculated as described in the experimental section (Table 1). As expected, the pK_a values decrease from **ST1** to **ST3**, due to the increase of the deactivating character of the substitutents in the position ortho to the hydroxy group. The pK_a value (3.4) of the dye **ST4** differs slightly from those estimated by Albuquerque and Calzaferri (3.7) [9].

3.2. Absorption and fluorescence spectra of the inserted cyanine dyes

All four dyes **ST1**—**ST4** were incorporated in the pores of zeolite L. Fig. 5 shows the remission and emission spectra of the dyes in

Table 1
Absorption (remission) and fluorescence maxima of acid and base forms in aqueous solution and in zeolite L, and calculated pK_a values in solution.

	Absorption/remission				Fluorescence				pK_a
	λ_{max} (acid form)		λ_{max} (base form)		λ_{max} (acid form)		λ_{max} (base form)		
	Solution	Zeolite L	Solution	Zeolite L	Solution	Zeolite L	Solution	Zeolite L	
ST1	370	368	444	–	505	501	580	–	8.6
ST2	375	381	460	–	609	492	611	–	6.8
ST3	359	369	435	–	455	458	582	589	5.0
ST4	330	333	450	–	408	394	610	595	3.4

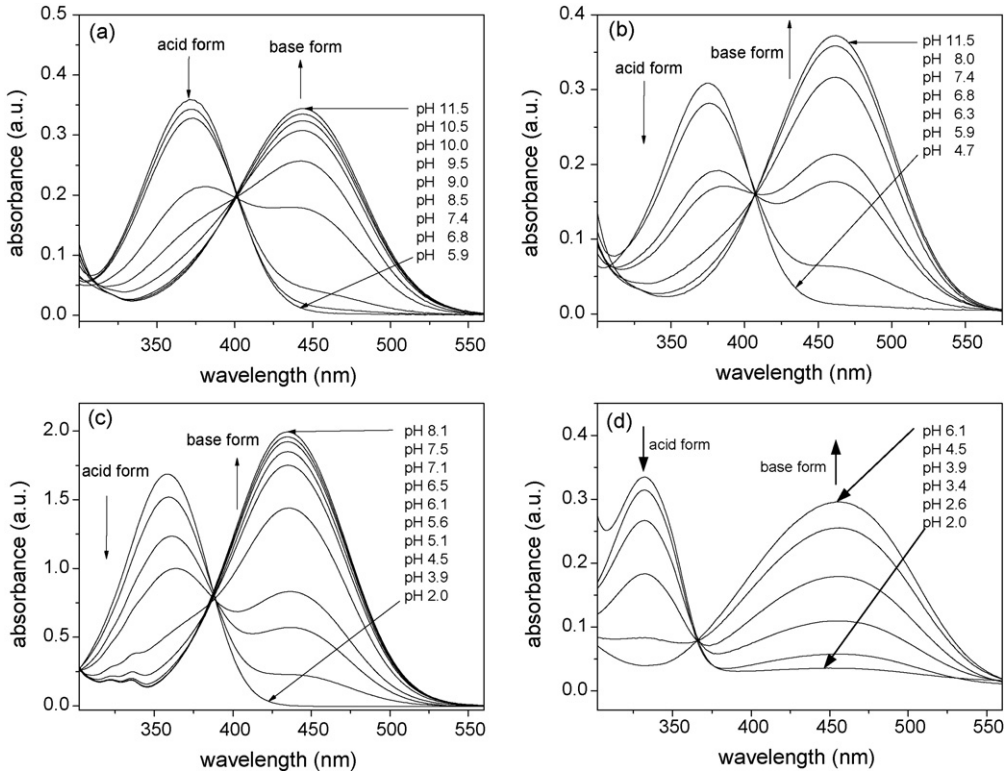

Fig. 3. Absorption spectra of (a) **ST1**, (b) **ST2**, (c) **ST3**, (d) **ST4** in aqueous buffered solutions of varying pH.

zeolite L. The remission spectra only show significant absorption of the acid form of the dyes while using more sensitive fluorescence spectroscopy, a significant contribution in fluorescence of the base form of dyes **ST3** and **ST4** (having lower pK_a values) is also observed.

Because of the rather weak emission of the deprotonated **ST3** in zeolite L we could only use the **ST4** spectrum to estimate the pore pH value in the zeolite L pores. The signal ratio of the acid to the base form of **ST4** in zeolite L is 3.63, and can only be used to roughly estimate the pH value inside the pore. Fig. 6 shows the fluorescence signal ratio of the acid and base forms of **ST4** in aqueous solutions of varying pH values as taken from Fig. 4d. With the data from the sigmoidal fit, and the signal ratio from the inserted dye, we estimated a pore pH value between 3.0 and 3.5. This is in quite good agreement to the value of 3.38 of Albuquerque and Calzaferri [9] for potassium exchanged zeolite L.

To estimate the polarity of the zeolite L pores, we investigated the solvatochromism of **ST3** in various solutions. The absorption spectra of the protonated and deprotonated forms, and the emission spectra of the deprotonated dye **ST3**, were recorded in six solvents with increasing polarity. While the absorption maxima of the protonated form shows no relation to the solvent polarity, the absorption maxima of the deprotonated compound shifts to shorter wavelengths with increasing solvent polarity (Table 2). The difference in the maxima between the least and the most polar solvent is 120 nm. Similarly the emission maxima show a negative solvatochromism but with a significantly smaller shift of 35 nm. When comparing the emission maximum of **ST3** in zeolite L (588 nm) with the solvent maxima (Table 2), we can deduce that the zeolite pores provide a medium of high polarity.

3.3. Reaction of the inserted ST3 with 1-propylamine

Fig. 7 shows the fluorescence spectra of the deprotonated **ST3** in zeolite L with different concentrations of 1-propylamine. Line

Table 2
Absorption and emission maxima of **ST3** in different solutions.

ST3	Absorption		Fluorescence
	λ_{max} (nm)		λ_{max} (nm)
	Acid form	Base form	Base form
Water	359	438	581
Methanol	371	484	592
Ethanol	376	509	597
1-Propanol	379	531	598
Dimethyl sulfoxide	370	536	614
Acetonitrile	362	537	613
Dimethylformamide	369	545	615
Acetone	366	559	615

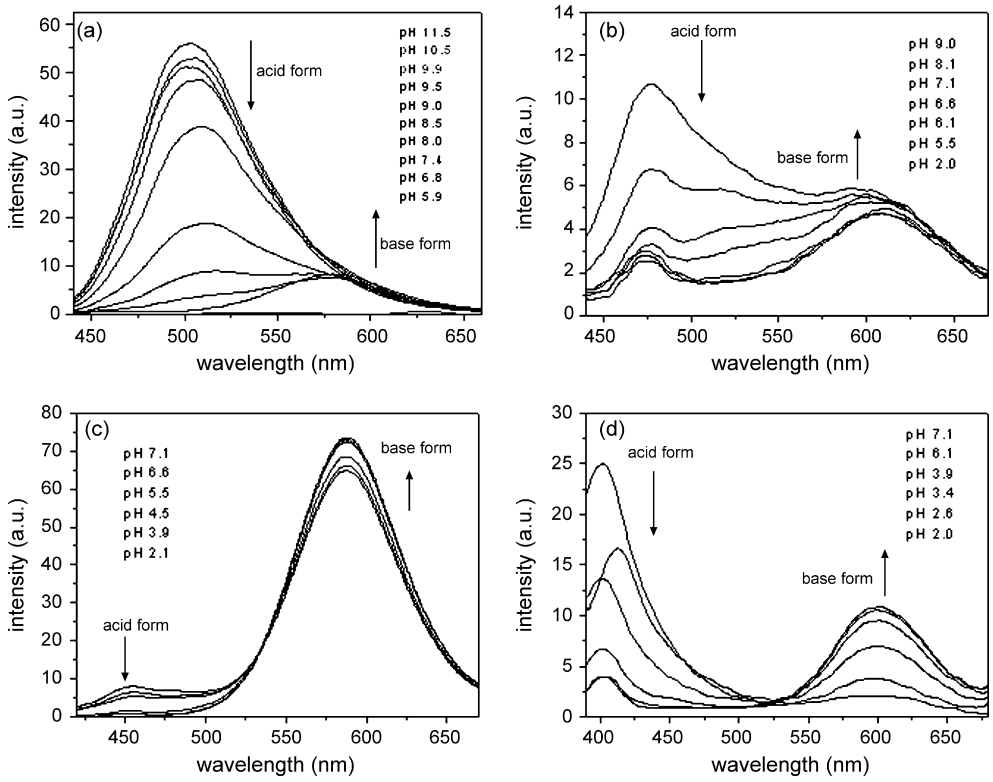

Fig. 4. Fluorescence spectra of (a) **ST1**, (b) **ST2**, (c) **ST3**, (d) **ST4** in aqueous buffered solutions of varying pH. Excitation set to the isosbestic point of the corresponding absorption spectra.

a shows the spectrum before treatment with amine. The fluorescence increases significantly with higher amine concentrations as expected for the low pK_a value of 5.0 (lines b to f). This sensitivity is a prerequisite for use of the dye–zeolite composites in optical sensors. However, we found that the time for reaching the equilibrium fluorescence signal was up to 2 h. Moreover, the time for the diffusion of the amine molecules out of the pores was extraordinary long and a complete removal could not be reached within a measure time of two days (line g). Thus, the use of this material is limited to applications as irreversible probes or test strips.

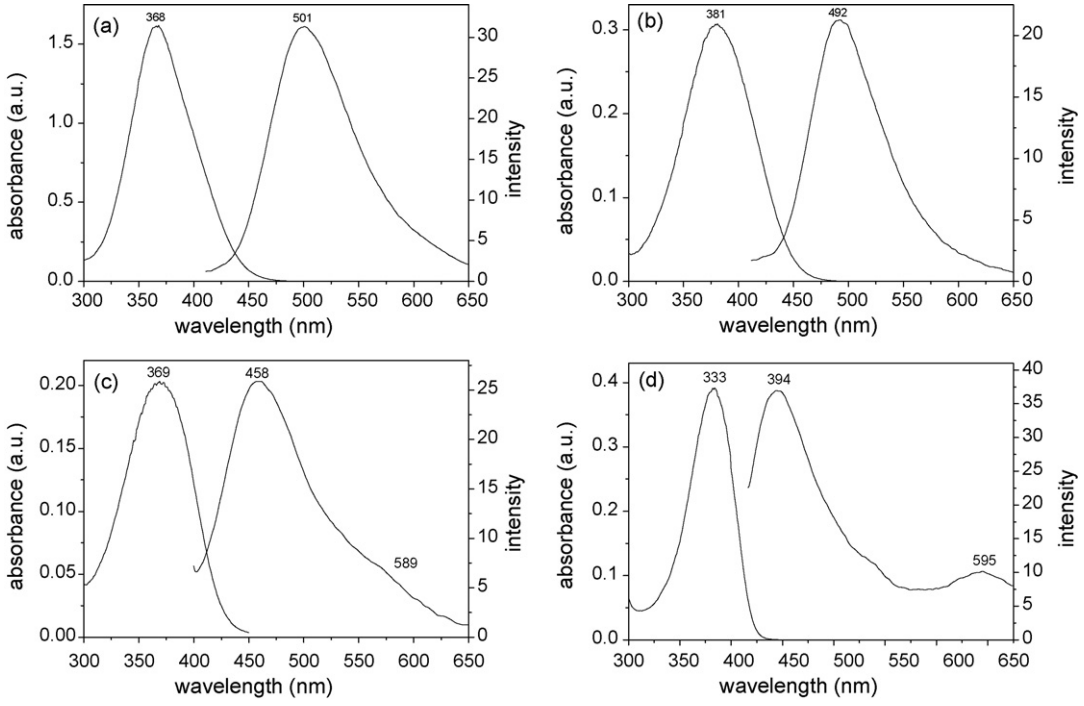

Fig. 5. Remission and fluorescence spectra of (a) **ST1**, (b) **ST2**, (c) **ST3**, (d) **ST4** in zeolite L.

Table 3
Bond distances and adsorption energies of the Brønstedt site of zeolite L in interaction with a pH sensitive dye.

	Z1			Z2		
	r (O–H)$_{zeolite}$ (Å)	r (O···H)$_{dye}$ (Å)	E_{ads} (kJ mol^{-1})	r (O–H)$_{zeolite}$ [Å]	r (O···H)$_{dye}$ (Å)	E_{ads} (kJ mol^{-1})
ST1	1.648	1.015	−132.6	1.702	1.005	−220.8
ST2	1.031	1.576	−94.0	1.009	1.661	−125.2
ST3	1.012	1.626	−103.2	1.004	1.713	−137.6
ST4	0.973	5.381 (N···H)	+5.5	0.984	3.405 (N···H)	−55.1
Bare	0.973			0.973		

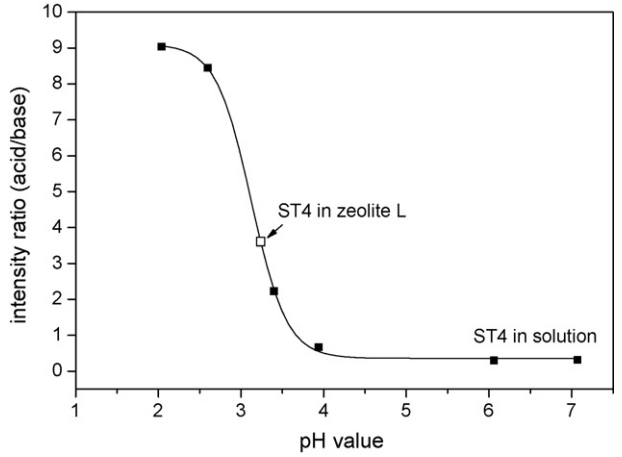

Fig. 6. Estimation of the pH value in zeolite L pores with **ST4**.

3.4. Quantum chemical calculations

Table 3 gives data from quantum chemical calculations of both the bare clusters **Z1** and **Z2,** and the clusters with an adsorbed dye. The bare clusters have a calculated O–H bond length of 0.973 Å. Together with the dyes **ST4** to **ST1** the zeolitic OH bond length elongates to 1.648 Å and 1.702 Å for the clusters **Z1** and **Z2**, respectively. On the other hand, the dye O–H (or N–H in case of **ST4**) bond lengths are decreased from **ST4** to **ST1**. Both these distances characterize the hydrogen bond strength and hence the zeolite acidity in this system. The less acidic the dye, the more it tends to deprotonate the acidic site at the zeolite. This result is in accordance with our experimental findings, in that the less acidic dyes (**ST1** and **ST2**) are completely protonated inside the pore, and only the both more acidic dyes (**ST3** and **ST4**) are partially protonated.

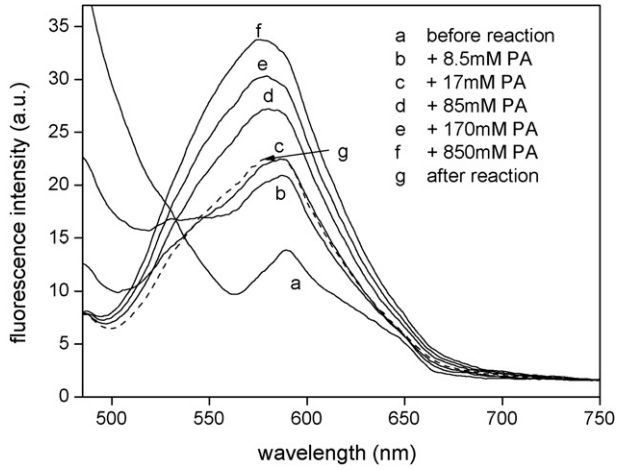

Fig. 7. Emission spectra of **ST3** at different 1-propylamine (PA) concentrations. The dashed line (g) shows the spectra after the reaction.

The adsorption energies were obtained by subtracting the total energies of the cluster (**Z1** or **Z2**) and the free dye molecules, from the total energy of the cluster with the dye adsorbed: $E_{ads} = E_{zeolite-dye} - E_{zeolite} - E_{dye}$. The adsorption energy arises from the hydrogen bonding and from the electrostatic and short-range interactions between the molecule and the zeolite framework. The final position of the molecule in the zeolite will depend on the local framework geometry and on the dye structure. The results in Table 3 indicate that E_{ads} is mainly governed by the strength of the hydrogen bond interaction. The system with the most acid dye, **ST4**, has the lowest adsorption energy (in the case of **Z1–ST4** it is even a positive value), while the system with the least acid dye, **ST1**, has the highest adsorption energy. The dye **ST2** has slightly lower E_{ads} values than **ST3**, indicating that other factors also influence the adsorption energies, such as electrostatic and short range interactions between the molecule and the zeolite framework.

4. Conclusion

We found that the pK_a value of cyanine dyes can be influenced by the substituents to give a wide range of pK_a values. Furthermore pH sensitive cyanine dyes are able to probe the acidity of the zeolite L pores, and since zeolite L exhibits a high proton activity and polarity, the dyes are mostly protonated. It is possible to use the functional zeolites for detecting gaseous amines. Quantum chemical calculations show that adsorption energies are mainly governed by the strength of the hydrogen bond interaction, and that other influences of weaker impact may be the electrostatic and short range interactions between the molecule and the zeolite framework.

Acknowledgements

This work was supported by the principal investigators fellowship MO 1062/6-1 and the project MO 1062/5-1 of Deutsche Forschungsgemeinschaft. This support is gratefully acknowledged. We would also like to thank Heidrun Müller for support in fluorescence measurements and Charles Cranfield for correction of the manuscript.

References

[1] M.K. Koo, C.H. Oh, A.L. Holme, S. Pervaiz, Cytometry A 71 (2007) 87.
[2] M.S. Briggs, D.D. Burns, M.E. Cooper, S.J. Gregory, Chem. Commun. (2000) 2323.
[3] H.A. Clark, M. Hoyer, M.A. Philbert, R. Kopelman, Anal. Chem. 71 (1999) 4831–4836.
[4] H.A. Clark, R. Kopelman, R. Tjalkens, M.A. Philbert, Anal. Chem. 71 (1999) 4837–4843.
[5] G. Schulz-Ekloff, D. Wöhrle, B. van Duffel, R. Schoonheydt, Micropor. Mesopor. Mater. 51 (2002) 91–138.
[6] G. Calzaferri, S. Huber, H. Maas, C. Minkowski, Angew. Chem. 115 (2003) 3860–3888.
[7] I. Braun, G. Ihlein, F. Laeri, J. Nöckel, G. Schulz-Ekloff, F. Schüth, U. Vietze, Ö. Weiss, D. Wöhrle, Appl. Phys. B: Lasers O 70 (2000) 335–343.
[8] B. Bussemer, D. Munsel, H. Wünscher, G.J. Mohr, U.-W. Grummt, J. Phys. Chem. B 111 (2007) 8–15.
[9] R.Q. Albuquerque, G. Calzaferri, Chem. Eur. J. 13 (2007) 8939–8952.
[10] G. Calzaferri, K. Lutkouskaya, Photochem. Photobiol. Sci. 7 (2008) 879–910.
[11] J.A. Ryder, A.K. Chakraborty, A.T. Bell, J. Phys. Chem. B 104 (2000) 6998–7011.
[12] M. Sierka, J. Sauer, J. Phys. Chem. B 105 (2001) 1603–1613.
[13] T. Baba, N. Komatsu, Y. Ono, J. Phys. Chem. B 102 (1998) 804–808.

[14] K. Sillar, P. Burk, J. Mol. Struct. THEOCHEM 281 (2002) 589–590.
[15] A. Simperler, R.G. Bell, M.D. Foster, A.E. Gray, D.W. Lewis, M.W. Anderson, J. Phys. Chem. B 108 (2004) 7152–7161.
[16] D.T. Chen, S.B. Sharma, I. Filimonov, J.A. Dumesic, Catal. Lett. 12 (1992) 201–212.
[17] (a) C.W. Chronister, R.S. Drago, J. Am. Chem. Soc. 115 (1993) 793–794;
(b) R.S. Drago, S.C. Dias, M. Torrealba, M.L. de Lima, J. Am. Chem. Soc. 119 (1997) 4444–4452.
[18] (a) M. Hunger, D. Freude, D. Fenzke, H. Pfeifer, Chem. Phys. Lett. 191 (1992) 391–395;
(b) P. Batamack, C. Doremieux-Morin, J. Fraissard, J. Chim. Phys. 89 (1992) 423–433.
[19] (a) W.H. Chen, H.H. Ko, A. Sakthivel, S.J. Huang, S.H. Liu, A.Y. Lo, T.C. Tsai, S.B. Liu, Catal. Today 116 (2006) 111–120;
(b) S.J. Huang, Y.H. Tseng, Y. Mou, S.B. Liu, S.H. Huang, C.P. Lin, J.C.C. Chan, Solid State Nucl. Magn. Reson. 29 (2006) 272–277;
(c) B. Alonso, I. Klur, D. Massiot, Chem. Commun. 8 (2002) 804–805.
[20] H.G. Karge, V. Dondur, J. Weitkamp, J. Phys. Chem. 95 (1991) 283–288.
[21] (a) N. Y: Topsøe, K. Pedersen, E.G. Derouane, J. Catal. 70 (1981) 41–52;
(b) P.A. Jacobs, J.A. Martens, J. Weitkamp, H.K. Beyer, Faraday Discuss. Chem. Soc. 72 (1981) 353–369;
(c) S. Narayanan, A. Sultana, Q. Thinh Le, A. Auroux, Appl. Catal. A 168 (1998) 373–384.
[22] F. Geobaldo, S. Fiorilli, B. Onida, G. Giordano, A. Katovic, E. Garrone, J. Phys. Chem. B 107 (2003) 1258–1262.
[23] (a) J.A. Lercher, C. Gründling, G. Eder-Mirth, Catal. Today 27 (1996) 353–376;
(b) L.M. Kustov, Top. Catal. 4 (1997) 131–144.
[24] G. Calzaferri, N. Gfeller, J. Phys. Chem. 96 (1992) 3428–3435.
[25] A. Zecchina, G. Spoto, S. Bordiga, Phys. Chem. Chem. Phys. 7 (2005) 1627–1642.
[26] (a) S. Corrent, P. Hahn, G. Pohlers, T.J. Connolly, J.C. Scaiano, V. Fornés, H. García, J. Phys. Chem. B 102 (1998) 5852–5858;
(b) S.Y. Choi, Y.S. Park, S.B. Hong, K.B. Yoon, J. Am. Chem. Soc. 118 (1996) 9377–9386.
[27] F. Lehmann, G.J. Mohr, U.-W. Grummt, Sensor. Actuat. B Chem. 38–39 (1997) 229–234.
[28] F. Lehmann, G.J. Mohr, P. Czerney, U.-W. Grummt, Dyes Pigm. 29 (1995) 85–94.
[29] M. Dbalska, I. Ruda, Can. J. Chem. 68 (1990) 691–695.
[30] K.J. Thomas, V. Ramamurthy, Langmuir 14 (1998) 6687–6692.
[31] K.F. Donchi, G.P. Rober, B. Ternai, P.J. Derrick, Aust. J. Chem. 33 (1980) 2199–2203.
[32] http://www.harrickscl.com/accessories/H_prayingmantis.cfm.
[33] M. J. Frisch, G. W. Trucks, H. B. Schlegel, G. E. Scuseria, M. A. Robb, J. R. Cheeseman, J. A. Montgomery, Jr., T. Vreven, K. N. Kudin, J. C. Burant, J. M. Millam, S. S. Iyengar, J. Tomasi, V. Barone, B. Mennucci, M. Cossi, G. Scalmani, N. Rega, G. A. Petersson, H. Nakatsuji, M. Hada, M. Ehara, K. Toyota, R. Fukuda, J. Hasegawa, M. Ishida, T. Nakajima, Y. Honda, O. Kitao, H. Nakai, M. Klene, X. Li, J. E. Knox, H. P. Hratchian, J. B. Cross, V. Bakken, C. Adamo, J. Jaramillo, R. Gomperts, R. E. Stratmann, O. Yazyev, A. J. Austin, R. Cammi, C. Pomelli, J. W. Ochterski, P. Y. Ayala, K. Morokuma, G. A. Voth, P. Salvador, J. J. Dannenberg, V. G. Zakrzewski, S. Dapprich, A. D. Daniels, M. C. Strain, O. Farkas, D. K. Malick, A. D. Rabuck, K. Raghavachari, J. B. Foresman, J. V. Ortiz, Q. Cui, A. G. Baboul, S. Clifford, J. Cioslowski, B. B. Stefanov, G. Liu, A. Liashenko, P. Piskorz, I. Komaromi, R. L. Martin, D. J. Fox, T. Keith, M. A. Al-Laham, C. Y. Peng, A. Nanayakkara, M. Challacombe, P. M. W. Gill, B. Johnson, W. Chen, M. W. Wong, C. Gonzalez, and J. A. Pople, Gaussian 03, Revision D.01, Gaussian, Inc., Wallingford CT (2004).